Optics Communications 424 (2018) 63–69

Contents lists available at ScienceDirect

Optics Communications

journal homepage: www.elsevier.com/locate/optcom

Generation of quadripartite entanglement from a hybrid scheme with a four-wave mixing process and linear beam splitters

Shuchao lv [a], Jietai Jing [a,b,c,*]

[a] State Key Laboratory of Precision Spectroscopy, East China Normal University, Shanghai 200062, China
[b] Department of Physics, Zhejiang University, Hangzhou 310027, China
[c] Collaborative Innovation Center of Extreme Optics, Shanxi University, Taiyuan, Shanxi 030006, China

ARTICLE INFO

MSC:
00-01
99-00

Keywords:
Quadripartite entanglement
Four-wave mixing process
$\mathcal{H}$-graph state

ABSTRACT

We theoretically propose a hybrid scheme with nonlinear four-wave mixing process and linear beam splitters to generate continuous-variable quadripartite entanglement. To expose the entanglement properties of the generated state, the coupling strength matrix is derived to reveal the interactions of the resulting modes at first. The generated state is verified to be a $\mathcal{H}$-graph state with a non-full rank coupling strength matrix by using graphical calculus for Gaussian pure states. Then based on the eigenmodes for the generated state, we find that the introduction of beam splitters does not alter the deduced eigenmodes of the nonlinear four-wave mixing process, and only contributes to generate quadripartite entanglement. In the end, we quantitatively investigate the internal entanglement structure of this scheme. Our work paves the way to generate quadripartite entanglement from a hybrid scheme with nonlinear four-wave mixing process and linear beam splitters.

1. Introduction

Multipartite entanglement, due to its unique properties, plays an important role not only in the field of testing quantum effects [1], but also in many applications, ranging from quantum information, quantum computing to quantum metrology. A large number of different schemes for generating multipartite entangled beams have already been theoretically proposed and experimentally implemented [2–8]. The usual technique depends on the interference of generated quadrature squeezed states [4]. The scalable optical quantum networks include the experimental generation of ultra-large-scale continuous variable (CV) cluster state multiplexed in both the time domain [9] and the frequency domain [10–12]. The standard method of generating CV entangled state is by parametric down-conversion in a nonlinear crystal, with an optical parametric oscillator (OPO). In this way, a very large amount of quantum correlation can be achieved. Recently, an alternative scheme to generate CV entanglement is to use the four-wave mixing (FWM) process in hot Rb vapor. In this scheme, the frequencies of the generated beams naturally match with the atomic ensembles. This feature is critical for achieving high efficiency quantum state mapping, storage, and retrieval for building future quantum networks [13]. In addition, the FWM process can be used to realize the quantum imaging due to its multi-spatial-mode nature [14]. This method is phase insensitive and single pass, hence it does not require any locking system. Due to these advantages, this system has found a variety of applications, such as the generation of tunable delay, low-noise amplification, and advancement of twin beams or entangled images [14–19]. It has been used as the fundamental element for a quantum interferometer, which can beat the standard quantum limit and approach the Heisenberg limit [20–22]. It has also been used to realize an ultrasensitive measurement of microcantilever displacement [23] and observe the localized multi-spatial-mode quadrature squeezing for quantum imaging [24].

Therefore, it is certainly worth developing the potential of the FWM process in hot Rb vapor as a competitive candidate for producing large-scale multipartite entangled states. Very recently, our group experimentally demonstrated a cascaded FWM process to produce multiple quantum correlated beams in hot rubidium vapor [25–27] and theoretically proposed a scheme to generate genuine multipartite entanglement [28,29]. A scheme to realize versatile quantum networks by cascading several FWM processes in warm rubidium vapors is also presented in Ref. [30].

Here we propose a hybrid scheme with nonlinear four-wave mixing process and linear beam splitters to generate CV quadripartite entanglement. It is theoretically verified that this scheme can generate quadripartite entanglement in the whole gain and transmission regions. Additionally, the quantitative analysis of quadripartite entanglement

* Corresponding author.
E-mail address: jtjing@phy.ecnu.edu.cn (J. Jing).

https://doi.org/10.1016/j.optcom.2018.04.031
Received 1 November 2017; Received in revised form 31 March 2018; Accepted 9 April 2018

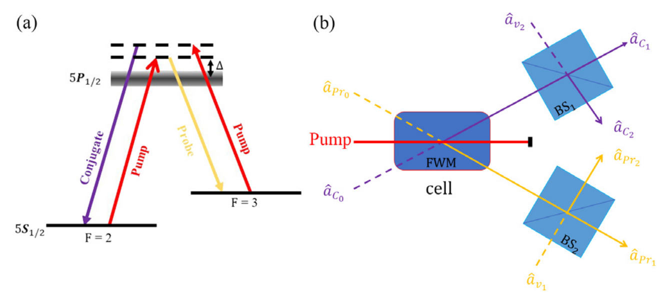

Fig. 1. Hybrid scheme for generating quadripartite entanglement. (a) Energy level diagram of ^{85}Rb *D1* line for the single FWM process, the width of the excited state $5P_{1/2}$ represents the Doppler broadening, and Δ represents the large detuning from the atomic transition. (b) Schematic view of our proposed scheme: Pr_0 and C_0 are vacuum inputs; Pr_1, Pr_2, C_1 and C_2 are resulting beams of second stage.

shows the symmetry of this scheme. The further properties are revealed by investigating the internal structure of entanglement, i.e., rule out one or more modes to analyze the genuine multipartite entanglement which potentially exists among the rest modes.

This paper is organized as follows. In Section 2, we begin with a brief introduction of a single FWM process and derive expressions for the output fields produced by this hybrid scheme. Then the adjacency matrix is extracted from the corresponding covariance matrix (CM) of the generated state [31]. It is verified that the generated state of our scheme is a $\mathcal{H}$-graph state. Then in Section 3, we proceed with a review of PPT criterion which we use to test the entanglement among Gaussian states from this system. In the following Section 4, we use PPT criterion to analyze the quadripartite entanglement, and investigate the entanglement structure. In Section 5, we give a brief summary of our results.

2. Hybrid scheme

Fig. 1(a) depicts the energy level diagram of a single FWM process in a hot rubidium vapor, where two pump photons can convert to a probe (signal) photon and a conjugate (idler) photon, or vice versa. The large detuning Δ of pump beam makes the frequencies of generated probe and conjugate beam lie outside the Doppler absorption profile [14]. As a result, the Doppler effect can be neglected in our analysis.

Fig. 1(b) shows how this hybrid scheme operates: a pair of twin beams are generated by the FWM process, then in the second stage, the twin beams are split by beams splitters BS$_1$ and BS$_2$ respectively. During the process in second stage, other two vacuum states $\hat{a}_{v_1}$ and $\hat{a}_{v_2}$ are introduced.

For an optical mode $\hat{a}$, $\hat{X}_a = \hat{a} + \hat{a}^\dagger$ and $\hat{Y}_a = (\hat{a} - \hat{a}^\dagger)/i$ stand for amplitude and phase quadrature, respectively. The commutation relation can be written as $[\hat{X}_a, \hat{Y}_a] = 2i$. The input–output relations of this scheme are

$$\hat{a}_{Pr_2} = \sqrt{\eta}(\sqrt{G}\hat{a}_{Pr_0} + \sqrt{g}\hat{a}^\dagger_{C_0}) + \sqrt{1-\eta}\hat{a}_{v_1}, \tag{1}$$

$$\hat{a}_{Pr_1} = \sqrt{1-\eta}(\sqrt{G}\hat{a}_{Pr_0} + \sqrt{g}\hat{a}^\dagger_{C_0}) - \sqrt{\eta}\hat{a}_{v_1}, \tag{2}$$

$$\hat{a}_{C_1} = \sqrt{1-\eta}(\sqrt{G}\hat{a}_{C_0} + \sqrt{g}\hat{a}^\dagger_{Pr_0}) - \sqrt{\eta}\hat{a}_{v_2}, \tag{3}$$

$$\hat{a}_{C_2} = \sqrt{\eta}(\sqrt{G}\hat{a}_{C_0} + \sqrt{g}\hat{a}^\dagger_{Pr_0}) + \sqrt{1-\eta}\hat{a}_{v_2}, \tag{4}$$

where the G is the power gain of the FWM process, $G - g = 1$, and η stands for the transmissions of BS$_1$ and BS$_2$ (the transmissions of these two BSs are set to be equal). Therefore, the modulo conventions of this scheme are

$$\begin{pmatrix} \hat{X}_{Pr_2} \\ \hat{X}_{Pr_1} \\ \hat{X}_{C_1} \\ \hat{X}_{C_2} \end{pmatrix} = \begin{pmatrix} \sqrt{\eta G} & \sqrt{\eta g} & \sqrt{1-\eta} & 0 \\ \sqrt{(1-\eta)G} & \sqrt{(1-\eta)g} & -\sqrt{\eta} & 0 \\ \sqrt{(1-\eta)g} & \sqrt{(1-\eta)G} & 0 & -\sqrt{\eta} \\ \sqrt{\eta g} & \sqrt{\eta G} & 0 & \sqrt{1-\eta} \end{pmatrix} \begin{pmatrix} \hat{X}_{Pr_0} \\ \hat{X}_{C_0} \\ \hat{X}_{v_1} \\ \hat{X}_{v_2} \end{pmatrix}, \tag{5}$$

and

$$\begin{pmatrix} \hat{Y}_{Pr_2} \\ \hat{Y}_{Pr_1} \\ \hat{Y}_{C_1} \\ \hat{Y}_{C_2} \end{pmatrix} = \begin{pmatrix} \sqrt{\eta G} & -\sqrt{\eta g} & \sqrt{1-\eta} & 0 \\ \sqrt{(1-\eta)G} & -\sqrt{(1-\eta)g} & -\sqrt{\eta} & 0 \\ -\sqrt{(1-\eta)g} & \sqrt{(1-\eta)G} & 0 & -\sqrt{\eta} \\ -\sqrt{\eta g} & \sqrt{\eta G} & 0 & \sqrt{1-\eta} \end{pmatrix} \begin{pmatrix} \hat{Y}_{Pr_0} \\ \hat{Y}_{C_0} \\ \hat{Y}_{v_1} \\ \hat{Y}_{v_2} \end{pmatrix}. \tag{6}$$

Eqs. (5) and (6) make it easy to calculate the covariances of modes' quadrature. Here, two modes' amplitude quadrature covariance is $\langle \hat{X}_j \hat{X}_k \rangle = \langle \hat{X}_j \hat{X}_k + \hat{X}_k \hat{X}_j \rangle/2 - \langle \hat{X}_j \rangle \langle \hat{X}_k \rangle$. A similar notation is applied to the phase quadrature, and $\langle \hat{X}_j \hat{Y}_k \rangle$ is zero in this scheme. Therefore, all the covariances of resulting beams are

$$\begin{aligned} &\langle \hat{X}^2_{Pr_2} \rangle = \langle \hat{Y}^2_{Pr_2} \rangle = \langle \hat{X}^2_{C_2} \rangle = \langle \hat{Y}^2_{C_2} \rangle = 2g\eta + 1, \\ &\langle \hat{X}^2_{Pr_1} \rangle = \langle \hat{Y}^2_{Pr_1} \rangle = \langle \hat{X}^2_{C_1} \rangle = \langle \hat{Y}^2_{C_1} \rangle = 2g(1-n) + 1, \end{aligned} \tag{7}$$

and

$$\begin{aligned} &\langle \hat{X}_{Pr_2} \hat{X}_{Pr_1} \rangle = \langle \hat{Y}_{Pr_2} \hat{Y}_{Pr_1} \rangle = 2g\sqrt{n(1-n)}, \\ &\langle \hat{X}_{Pr_2} \hat{X}_{C_1} \rangle = -\langle \hat{Y}_{Pr_2} \hat{Y}_{C_1} \rangle = 2\sqrt{Ggn(1-n)}, \\ &\langle \hat{X}_{Pr_2} \hat{X}_{C_2} \rangle = -\langle \hat{Y}_{Pr_2} \hat{Y}_{C_2} \rangle = 2n\sqrt{Gg}, \\ &\langle \hat{X}_{Pr_1} \hat{X}_{C_1} \rangle = -\langle \hat{Y}_{Pr_1} \hat{Y}_{C_1} \rangle = 2(1-n)\sqrt{Gg}, \\ &\langle \hat{X}_{Pr_1} \hat{X}_{C_2} \rangle = -\langle \hat{Y}_{Pr_1} \hat{Y}_{C_2} \rangle = 2\sqrt{Ggn(1-n)}, \\ &\langle \hat{X}_{C_1} \hat{X}_{C_2} \rangle = \langle \hat{Y}_{C_1} \hat{Y}_{C_2} \rangle = 2g\sqrt{n(1-n)}. \end{aligned} \tag{8}$$

It is straightforward to see that the power gain G and transmission η both affect the covariances in our scheme. To analyze the internal interactions of modes, we calculate the eigenmodes of generated states. From the Ref. [30], the eigenvalues of the FWM process in first stage are $\nu_+ = (\sqrt{G} + \sqrt{g})^2$ and $\nu_- = (\sqrt{G} - \sqrt{g})^2$. It can be verified that the values of eigenmodes are not altered after the second stage is introduced, but two vacuum states are introduced. This is due to the fact that two BSs do not introduce extra nonlinear quantum correlation.

Then we use the graphical calculus for Gaussian pure states to derive the adjacency matrix of the generated state. The corresponding adjacency matrix Z of this generated state is

$$Z = i\begin{bmatrix} 1+2\eta g & 2g\sqrt{\eta(1-\eta)} & -2\sqrt{Gg\eta(1-\eta)} & -2\eta\sqrt{Gg} \\ 2g\sqrt{\eta(1-\eta)} & -1+2\eta+2G(1-n) & -2(1-\eta)\sqrt{Gg} & -2\sqrt{Gg\eta(1-\eta)} \\ -2\sqrt{Gg\eta(1-\eta)} & -2(1-\eta)\sqrt{Gg} & -1+2\eta+2G(1-n) & 2g\sqrt{\eta(1-\eta)} \\ -2\eta\sqrt{Gg} & -2\sqrt{Gg\eta(1-\eta)} & 2g\sqrt{\eta(1-\eta)} & 1+2\eta g \end{bmatrix}. \tag{9}$$

From Z, we conclude that this generated state yields a graph where all the nodes are connected within each other, and with weights that vary and depend on the G and η. Additionally, the purely imaginary adjacency matrix Z can correspond to a $\mathcal{H}$-graph state, if there exists a real, symmetric matrix A such that $Z = ie^{-2\alpha A}$ is satisfied ($\cosh\alpha = \sqrt{G}$) [31]. We verify the generated state is a $\mathcal{H}$-graph state since A is

$$A = \begin{bmatrix} 0 & 0 & \sqrt{\eta(1-\eta)} & \eta \\ 0 & 0 & \sqrt{(1-\eta)} & \sqrt{\eta(1-\eta)} \\ \sqrt{\eta(1-\eta)} & \sqrt{(1-\eta)} & 0 & 0 \\ \eta & \sqrt{\eta(1-\eta)} & 0 & 0 \end{bmatrix}. \tag{10}$$

This result not only contributes to verify that the generated state is a $\mathcal{H}$-graph state, but also help reveal the internal interactions of the generated modes. Since aforementioned Hamiltonian is of the form

$$\mathcal{H} = i\hbar\alpha A_{jk}(\hat{a}^\dagger_j \hat{a}^\dagger_k - \hat{a}_j \hat{a}_k) \tag{11}$$

where A_{jk} denotes the interaction of two fields.

Additionally, the coupling strengths matrix is verified to be non-full rank. Therefore, the generated state cannot correspond to a CV cluster state in the limits of large power gain with phase shift operations [31,32]. These results are to be expected, since the introduction of second stage does not alter the essence of FWM process.

After having assessed the generated state is a $\mathcal{H}$-graph state, and exposed the internal interactions among the generated modes, we